

ARTICLE **OPEN**

LncRNA KIAA0087 suppresses the progression of osteosarcoma by mediating the SOCS1/JAK2/STAT3 signaling pathway

Haoli Gong¹, Ye Tao², Sheng Xiao¹, Xin Li¹, Ke Fang¹, Jie Wen¹, Pan He¹ and Ming Zeng¹✉

© The Author(s) 2023

Long noncoding RNAs (lncRNAs), widely expressed in mammalian cells, play pivotal roles in osteosarcoma (OS) progression. Nevertheless, the detailed molecular mechanisms of lncRNA KIAA0087 in OS remain obscure. Here, the roles of KIAA0087 in OS tumorigenesis were investigated. KIAA0087 and miR-411-3p levels were detected by RT-qPCR. Malignant properties were assessed by CCK-8, colony formation, flow cytometry, wound healing, and transwell assays. SOCS1, EMT, and JAK2/STAT3 pathway-related protein levels were measured by western blotting. Direct binding between miR-411-3p and KIAA0087/SOCS1 was validated by a dual-luciferase reporter, RIP, and FISH assays. In vivo growth and lung metastasis were evaluated in nude mice. The expression levels of SOCS1, Ki-67, E-cadherin, and N-cadherin in tumor tissues were measured by immunohistochemical staining. Downregulation of KIAA0087 and SOCS1 and upregulation of miR-411-3p were found in OS tissues and cells. Low expression of KIAA0087 was associated with a poor survival rate. Forced expression of KIAA0087 or miR-411-3p inhibition repressed the growth, migration, invasion, EMT, and activation of the JAK2/STAT3 pathway and triggered apoptosis of OS cells. However, the opposite results were found with KIAA0087 knockdown or miR-411-3p overexpression. Mechanistic experiments indicated that KIAA0087 enhanced SOCS1 expression to inactivate the JAK2/STAT3 pathway by sponging miR-411-3p. Rescue experiments revealed that the antitumor effects of KIAA0087 overexpression or miR-411-3p suppression were counteracted by miR-411-3p mimics or SOCS1 inhibition, respectively. Finally, in vivo tumor growth and lung metastasis were inhibited in KIAA0087-overexpressing or miR-411-3p-inhibited OS cells. In summary, the downregulation of KIAA0087 promotes the growth, metastasis, and EMT of OS by targeting the miR-411-3p-mediated SOCS1/JAK2/STAT3 pathway.

Experimental & Molecular Medicine (2023) 55:831–843; <https://doi.org/10.1038/s12276-023-00972-8>

INTRODUCTION

Osteosarcoma (OS) is a bone malignancy that most commonly occurs in children and adolescents¹. Globally, 4–5 per million patients are diagnosed with OS annually². The current treatments for OS are surgery in combination with chemotherapy or radiotherapy as well as administration of novel antitumor agents or molecularly targeted therapies³. Nevertheless, the 5-year survival rate for OS patients is between 40% and 70%^{2,4}, which can decline to only 19% when metastasis occurs⁵. With increasing research on the pathogenesis of OS, much attention has been given to epithelial-mesenchymal transition (EMT). EMT is a transformation of polarized epithelial cells to mesenchymal cells⁶. EMT drives the tumorigenesis and progression of OS by enhancing the metastatic ability of cancer cells⁷. Due to the promotive roles of EMT in OS progression, inhibition of EMT has been considered a promising therapeutic strategy.

Long noncoding RNA (lncRNA), a novel kind of noncoding RNA, is composed of more than 200 nucleotides without coding potential. Abnormal expression of certain lncRNAs is significantly associated with the malignant phenotypes of tumor cells⁸. A previous study revealed that lncRNA KIAA0087 levels were reduced in endometrial carcinoma and participated in endometrial carcinogenesis⁹. To date, the expression and functional roles of KIAA0087 in OS have not been revealed. A new theory that

lncRNAs may counteract the biological activities of microRNAs (miRNAs) by sponging them has been widely accepted¹⁰. MiRNAs are another kind of noncoding RNA composed of 17–25 nucleotides; these RNAs repress the translation of target genes by complementary base pairing, and this function of miRNAs has been shown to be involved in the pathogenesis of tumors¹¹. Many differentially expressed miRNAs have been documented to regulate the malignancy of OS cells^{12,13}. Recently, one study reported the upregulation of miR-411-3p in OS cell lines¹⁴. However, the functional roles of dysregulated miR-411-3p in OS are unclear. Importantly, bioinformatics analysis (based on the LncBase database) shows that KIAA0087 can bind to miR-411-3p, although no studies have reported an interaction between them. Therefore, KIAA0087 might affect OS progression by regulating miR-411-3p expression.

The suppressor of cytokine signaling 1 (SOCS1) is a member of the SOCS family. SOCS1 is considered a suppressor or promotor of different cancers¹⁵. A reduced SOCS1 level mediated by promoter methylation has been shown to facilitate EMT and the development of acute myeloid leukemia cells by activating the JAK2/STAT3 signaling pathway¹⁶. In contrast, another study demonstrated that SOCS1 deficiency slowed tumor development by increasing antitumor inflammation¹⁷. To date, only one study has indicated that SOCS1 methylation confers malignant properties to OS cells¹⁸. Notably, based on the StarBase database,

¹Department of Orthopedics, Hunan Provincial People's Hospital (The First Affiliated Hospital of Hunan Normal University), Changsha 410005 Hunan Province, P. R. China.

²Department of Radiology, The Third Xiangya Hospital, Central South University, Changsha 410013 Hunan Province, P. R. China. ✉email: 15570861867@hunnu.edu.cn

Received: 26 April 2022 Revised: 16 November 2022 Accepted: 3 January 2023

Published online: 3 April 2023

SOCS1 is predicted to be a target of miR-411-3p. Therefore, the miR-411-3p/SOCS1 axis might participate in KIAA0087-regulated OS progression.

In this study, we found decreased KIAA0087 and elevated miR-411-3p expression in OS tissues and cells, which contributed to the proliferation, migration, invasion, and EMT of OS cells. KIAA0087 sponged miR-411-3p to enhance SOCS1 expression and subsequently suppressed JAK2/STAT3 pathway-mediated EMT. Our study suggested the potential of KIAA0087 as a novel target and prognostic indicator for OS.

MATERIALS AND METHODS

Clinical samples

Clinical OS tissues and matched normal tissues were collected from 30 OS patients during surgery at Hunan Provincial People's Hospital (The First Affiliated Hospital of Hunan Normal University). The collected samples were snap-frozen in liquid nitrogen and preserved at -80°C . None of the patients had previously undergone chemoradiotherapy, and all the patients signed written informed consent. Our experiments were approved by the Ethics Committee of Hunan Provincial People's Hospital (The First Affiliated Hospital of Hunan Normal University). Table 1 presents the clinicopathological characteristics of these patients.

Cells and treatment

OS cells (U2OS, Saos-2, MG-63, and HOS) and human osteoblasts (hFOB 1.19) were obtained from the Cell Bank of the Chinese Academy of Science (Shanghai, China). U2OS (MEM, Gibco, Grand Island, NY, USA), Saos-2 (MEM, Gibco), MG-63 (McCoy's 5A, Gibco), HOS (McCoy's 5A, Gibco), and hFOB 1.19 (DMEM, Gibco) cells were cultured in an appropriate medium containing 10% fetal bovine serum (FBS, Gibco) and 1% penicillin/streptomycin (Invitrogen, CA, USA) and incubated at 37°C with 5% CO_2 .

Lentivirus infection

The lentivirus vector used to overexpress KIAA0087 (OE-KIAA0087), short hairpin RNA used to silence KIAA0087 and SOCS1 (sh-KIAA0087 and sh-SOCS1), their negative controls (OE-NC and sh-NC), miR-411-3p mimics, miR-411-3p inhibitor, and mimics/inhibitor NC were purchased from GeneChem (Shanghai, China). U2OS and Saos-2 cells were infected with the above lentiviruses with $5\ \mu\text{g}/\text{mL}$ polybrene (GeneChem).

Cell counting kit-8 (CCK-8)

The proliferation of OS cells was assessed at various time points (24, 48, and 72 h) with a CCK-8 Kit (Bestbio, Shanghai, China) strictly in accordance

with the manufacturer's instructions. The results were obtained using a multimode reader at 450 nm (Tecan, Männedorf, Switzerland).

Colony formation assay

The proliferation of OS cells was evaluated by colony formation. After culturing 100 cells in 6-well plates for 2 weeks, the clones were fixed with 4% paraformaldehyde and stained with 0.5% crystal violet solution. Subsequently, the colony number was calculated.

Cell apoptosis detection

An Annexin V-FITC/PI Apoptosis Detection Kit (Thermo Fisher Scientific) was adopted for apoptosis detection. Briefly, OS cells were stained with Annexin V-FITC (5 μL) and PI Staining Solution (10 μL). After a reaction for 10 min in the dark, 400 μL binding buffer was added, followed by detection by flow cytometry (Becton-Dickinson).

Wound healing assay

The migration of OS cells was determined by wound healing assay. A scratch was made in confluent OS cells seeded in 24-well plates using a micropipette tip. Then, the cells were permitted to migrate in a serum-free medium for 24 h. The cells were imaged with a microscope (Zeiss, Germany) at 0 and 24 h after scratch treatment.

Transwell assay

OS cells in 200 μL serum-free medium were added to the upper chamber of a transwell system coated with Matrigel (BD Biosciences, San Jose, CA, USA). The lower chamber was filled with 600 μL medium containing 10% FBS. After invading for 24 h in an incubator, the noninvaded cells in the upper chamber were removed by swabbing, and the invaded cells on the lower surface of the chamber were fixed in 4% paraformaldehyde, stained with 0.5% crystal violet, and photographed under a microscope (Zeiss, Germany).

Dual-luciferase reporter assay

The interaction between KIAA0087 and miR-411-3p was predicted using the LncBase database (http://carolina.imis.athena-innovation.gr/diana_tools/web/index.php?r=lnccbasev2/index-predicted). The direct binding between the SOCS1 3'-UTR and miR-411-3p was predicted using the StarBase database (<http://starbase.sysu.edu.cn/index.php>). The sequences of wild-type (WT) KIAA0087 and SOCS1 3'-UTR containing miR-411-3p binding sites or the mutant (MUT) sequences were obtained by PCR amplification and subcloned into the psiCHECK2 vector (Promega, Madison, Wisconsin, USA). OS cells were cotransfected with KIAA0087-WT, SOCS1-WT, or SOCS1-MUT vectors with miR-411-3p mimics or inhibitors. Subsequently, the luciferase

Table 1. Associations between KIAA0087/miR-411-3p expression and clinicopathological characteristics in osteosarcoma patients.

Clinical parameter	Cases (n)	Expression level		P value	Expression level		P value
		KIAA0087 ^{high}	KIAA0087 ^{low}		miR-411-3p ^{high}	miR-411-3p ^{low}	
<i>Age (years)</i>							
<18 years	20	9	11	0.6999	12	8	0.2451
≥ 18 years	10	6	4		3	7	
<i>Sex</i>							
Male	17	7	10	0.4621	8	9	1.0000
Female	13	8	5		7	6	
<i>Tumor size (cm)</i>							
<5 cm	12	9	3	0.0604	5	7	0.7104
≥ 5 cm	18	6	12		10	8	
<i>TNM stage</i>							
I	14	12	2	0.0007	4	10	0.0656
II + III	16	3	13		11	5	
<i>Distant metastasis</i>							
Yes	16	7	9	0.7152	12	4	0.0092
NO	14	8	6		3	11	

activity of OS cells was assessed with a Dual-Lucy Assay Kit (Solarbio, Beijing, China) after 48 h.

RNA immunoprecipitation (RIP) assay

A Magna RIP RNA-Binding Protein Immunoprecipitation Kit (Millipore, Billerica, MA, USA) was used after OS cells were transfected with miR-411-3p mimics or NC mimics. Magnetic beads conjugated to Ago2 (Millipore) or nonspecific IgG antibody (Millipore) were applied for incubation with cell lysates at 4 °C overnight. After treatment with proteinase K, the level of KIAA0087 in the immunoprecipitated RNAs was assessed by qPCR.

Fluorescence in situ hybridization (FISH) assay

Cy3-labeled KIAA0087 and FITC-labeled miR-411-3p probes were purchased from GenePharma (Shanghai, China). The probe signals were determined with a FISH Probe Kit from GenePharma. Nuclei were stained with DAPI (Solarbio). The co-localization of KIAA0087 and miR-411-3p in OS cells was observed under a fluorescence microscope (Zeiss, Germany).

Animal studies

The animal experiments were approved by the Animal Ethics Committee of Hunan Provincial People's Hospital (The First Affiliated Hospital of Hunan Normal University, IRB number: 20210021). Six-week-old male BALB/C nude mice were purchased from Shanghai SLAC Laboratory Animal Center (Shanghai, China). For the tumorigenesis experiment, mice have subcutaneously injected with 1×10^7 U2OS or Saos-2 cells stably infected with lentiviruses carrying KIAA0087 or miR-411-3p inhibitor ($n = 6$ per group). All mice were sacrificed 30 days after injection, and the xenograft tumors were collected and weighed.

For the metastasis experiment, the mice were injected via the tail vein with 5×10^6 U2OS or Saos-2 cells stably infected with lentiviruses carrying KIAA0087 or miR-411-3p inhibitor. Four weeks later, all mice were sacrificed, and lung metastasis was evaluated. The obtained lung tissues were fixed in 10% formalin for subsequent experiments.

Hematoxylin and eosin (H&E) staining

For lung metastasis analysis, the lung tissues of nude mice were subjected to paraffin embedding and cut into 5 μ m-thick serial sections, stained with H&E solution (Abcam), and photographed under a light microscope (Zeiss, Germany).

Immunohistochemical staining

The prepared paraffin sections were dewaxed, rehydrated, and incubated in 3% H₂O₂. Then, antigen retrieval was performed by heating in citrate buffer. The sections were probed with primary antibodies against SOCS1 (1:200, ab9870, Abcam), Ki-67 (1:500, ab15580, Abcam), E-cadherin (1:400, #3195, Cell Signaling Technology, Danvers, MA, USA), and N-cadherin (1:100, #13116, Cell Signaling Technology) overnight at 4 °C. Thereafter, the biotinylated secondary antibody was applied, followed by visualization with 3,3'-diaminobenzidine (DAB).

Western blot analysis

Protein isolation from OS cells was carried out using RIPA buffer (Beyotime, Shanghai, China) containing a proteinase inhibitor cocktail. Total protein was quantified with the BCA Protein Assay Kit (Beyotime); proteins were then separated by SDS-PAGE and transferred onto polyvinylidene fluoride membranes (Millipore). The primary antibodies for immunoblotting were as follows: E-cadherin (1:1000, #3195, Cell Signaling Technology), N-cadherin (1:2000, #13116, Cell Signaling Technology), vimentin (1:1500, #5741, Cell Signaling Technology), MMP-2 (1:1000, #40994, Cell Signaling Technology), slug (1:1000, #9585, Cell Signaling Technology), SOCS1 (1:2000, ab62584, Abcam), p-JAK2 (Tyr1007, 1:1000, #4406, Cell Signaling Technology), JAK2 (1:1500, #3230, Cell Signaling Technology), p-STAT3 (Tyr705, 1:1000, ab267373, Abcam), STAT3 (1:1000, ab68153, Abcam), bax (1:2000, ab182733, Abcam), bcl-2 (1:2000, ab182858, Abcam), cleaved caspase-3 (1:500, ab2302, Abcam), Notch1 (1:1000, ab52627, Abcam), Hes1 (1:1000, ab71559, Abcam), β -catenin (1:1000, ab223075, Abcam), c-Myc (1:1000, #13987, Cell Signaling Technology), p-P13K (Tyr607, 1:1000, ab182651, Abcam), P13K (1:1000, ab191606, Abcam), p-AKT (Ser473, 1:2000, #4060, Cell Signaling Technology), AKT (1:1000, #4691, Cell Signaling Technology), and GAPDH (1:2000, ab9485, Abcam). These antibodies were applied at 4 °C overnight. After incubation with the secondary antibody, the protein bands were detected using ECL substrate (Thermo Fisher Scientific).

Real-time quantitative PCR (RT-qPCR)

Total RNA was isolated using the TRIzol RNA Extraction Kit (Engreen Biosystem, Birkenhead, Auckland, New Zealand). Reverse transcription was carried out using the PrimeScript RT Reagent Kit gDNA Eraser (Takara, Dalian, China). The relative expression levels of KIAA0087, SOCS1, RHOB, XRN1, miR-411-3p, miR-30e-5p, miR-135b-5p, miR-6807-3p, and miR-488-3p were determined by qPCR using the SYBR Premix Ex Taq II Kit (TaKaRa). GAPDH and U6 small nuclear RNA were used as internal references for mRNA and miRNA, respectively. The relative quantification of gene expression was determined using the $2^{-\Delta\Delta C_t}$ method.

Statistical analysis

Data from three biological replicates were analyzed with GraphPad Prism 6.0 and are presented as the mean \pm standard deviation (SD). Student's *t*-test was performed when there were two experimental groups, while a one-way analysis of variance (ANOVA) followed by Tukey's post hoc test was performed for multiple group comparisons. The overall survival curve of OS patients was analyzed with the Kaplan–Meier method. Spearman correlation analysis was used to study the relationship between KIAA0087, miR-411-3p, and SOCS1. The correlation between KIAA0087 and miR-411-3p expression and the clinicopathological characteristics of OS patients was assessed with the chi-square test. A *P* value less than 0.05 was considered significant.

RESULTS

Downregulation of KIAA0087 indicates a poor prognosis and activates the JAK2/STAT3 pathway in OS

KIAA0087 is a novel lncRNA, and its biological functions in OS remain unclear. We first investigated the expression level of KIAA0087 in OS tissues and cells using RT-qPCR. Significant downregulation of KIAA0087 was found in OS tissues (Fig. 1a), and a series of OS cells (Fig. 1b) compared to the corresponding control groups. Moreover, the survival rate was decreased in patients with lower expression of KIAA0087 than in those with high expression of KIAA0087 (Fig. 1c). To further explore the functional roles of KIAA0087 in EMT, we evaluated the effects of KIAA0087 on EMT-related signaling pathways (JAK2/STAT3, Notch1/Hes1, and Wnt/ β -catenin). KIAA0087 was overexpressed or silenced in U2OS and Saos-2 cells (Fig. 1d). The phosphorylation levels of JAK2 and STAT3 were reduced, while the SOCS1 level was enhanced in U2OS and Saos-2 cells after forced expression of KIAA0087. However, the opposite results were found with the loss of KIAA0087 (Fig. 1e). As presented in Supplementary Fig. 1a, b, the expression levels of Notch1, Hes1, β -catenin, and c-Myc in OS cells were not changed after overexpression or knockdown of KIAA0087. Taken together, KIAA0087 was expressed at low levels in OS, which was correlated with a poor prognosis and dysregulation of the JAK2/STAT3 pathway.

KIAA0087 affects the proliferation and apoptosis of OS cells

Further functional assays indicated that forced expression of KIAA0087 strikingly repressed the growth of both U2OS and Saos-2 cells, while the opposite results were found with the knockdown of KIAA0087 (Fig. 2a, b). In addition, the apoptosis of OS cells was induced by KIAA0087 overexpression but inhibited by its depletion (Fig. 2c). As assessed by western blotting, overexpression of KIAA0087 resulted in upregulation of Bax and cleaved caspase-3 and downregulation of bcl-2 in OS cells, whereas KIAA0087 deficiency led to the opposite results (Fig. 2d). These findings suggested that KIAA0087 repressed the proliferation and induced the apoptosis of OS cells.

KIAA0087 suppresses the migration, invasion, and EMT of OS cells

The migration and invasion of OS cells were remarkably suppressed in KIAA0087-overexpressing OS cells but enhanced in KIAA0087-silenced cells (Fig. 3a, b). Thus, we speculated that the EMT process might be regulated by KIAA0087. As detected by

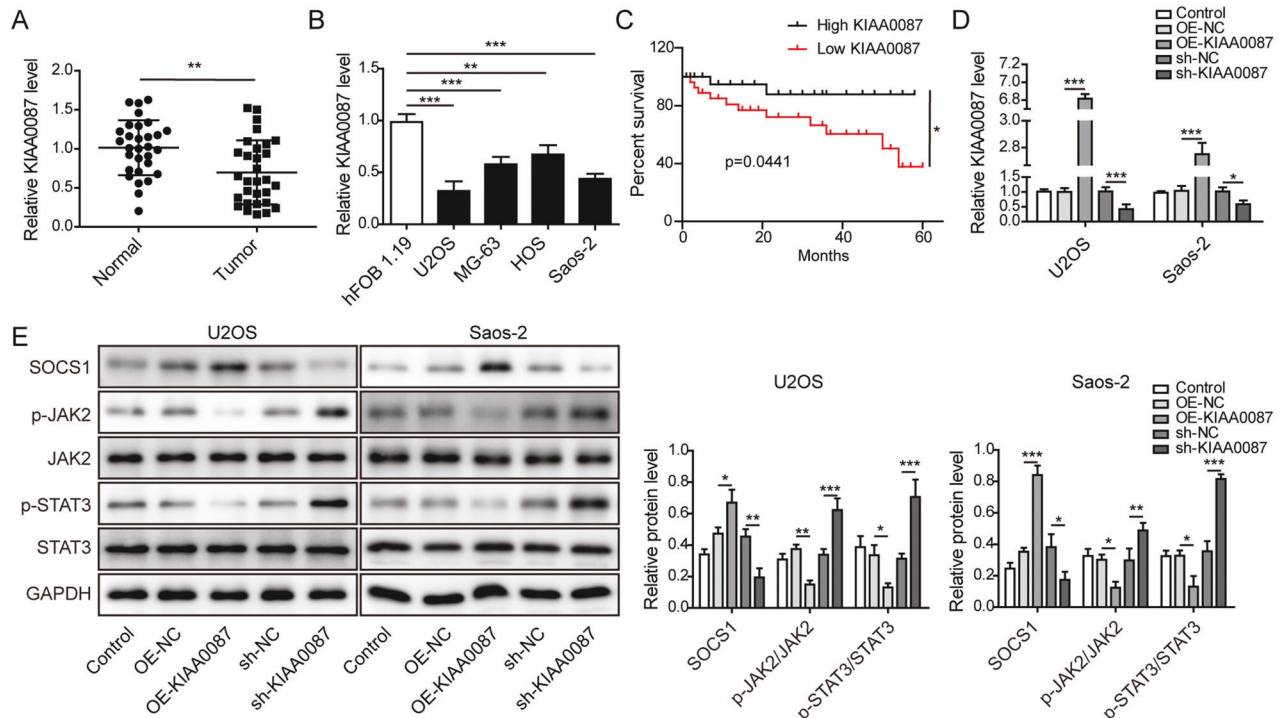


Fig. 1 Aberrant low expression of KIAA0087 in OS is associated with a poor prognosis. **a** RT-qPCR analysis was used to evaluate KIAA0087 levels in clinically normal and OS samples ($n = 30$). **b** RT-qPCR analysis was used to evaluate KIAA0087 levels in hFOB 1.19 and different OS cells (U2OS, Saos-2, MG-63, and HOS). **c** The survival rate of OS patients with high or low expression of KIAA0087. **d** The transfection efficiency of overexpression or silencing of KIAA0087 was detected by RT-qPCR. **e** Western blot analysis of the protein levels of SOCS1, p-JAK2, JAK2, p-STAT3, and STAT3. * $p < 0.05$, ** $p < 0.01$, and *** $p < 0.001$.

western blotting, KIAA0087 overexpression increased E-cadherin expression but decreased N-cadherin, vimentin, MMP-2, and slug expression in OS cells, suggesting the inhibition of EMT. However, KIAA0087 depletion exhibited the opposite effects (Fig. 3c). Collectively, the above findings suggested that the abnormal downregulation of KIAA0087 endowed OS cells with migration, invasion, and EMT abilities.

KIAA0087 directly interacts with miR-411-3p in OS cells

As predicted by bioinformatics analysis, five target miRNAs (miR-411-3p, miR-30e-5p, miR-135b-5p, miR-6807-3p, and miR-488-3p) of KIAA0087 were screened according to prediction ranking and research status. Furthermore, RT-qPCR results showed that the change in miR-411-3p level was apparently most pronounced among the above five miRNAs after overexpression or knockdown of KIAA0087 in OS cells (Fig. 4a). Furthermore, miR-411-3p was negatively correlated with KIAA0087 levels in OS tissues (Fig. 4b). The LncBase database predicted that miR-411-3p was a potential target of KIAA0087 (Fig. 4c). The relative luciferase activity of the KIAA0087-WT group was dramatically reduced by miR-411-3p mimics but increased by the miR-411-3p inhibitor. However, there were no significant changes in the KIAA0087-MUT groups (Fig. 4d). Additionally, the RIP assay confirmed the direct interaction of miR-411-3p with KIAA0087 (Fig. 4e). FISH assays further demonstrated the colocalization of KIAA0087 and miR-411-3p in the cytoplasm of OS cells (Fig. 4f). Thus, KIAA0087 could bind to miR-411-3p and negatively regulate its expression in OS.

Upregulation of miR-411-3p confers OS cell growth and proliferation

Since KIAA0087 could sponge miR-411-3p and repress miR-411 expression in OS cells, we further focused on the expression and functional roles of miR-411-3p in OS. We observed that miR-411-

3p was evidently upregulated in OS tissues (Fig. 5a) and a panel of OS cells (Fig. 5b). Next, the transfection efficiency of miR-411-3p in OS cells was verified by RT-qPCR (Fig. 5c). Functional experiments showed that the miR-411-3p inhibitor restricted growth and promoted apoptosis of OS cells. In contrast, miR-411-3p overexpression promoted growth and proliferation and inhibited apoptosis of OS cells (Fig. 5d-f). In addition, the protein levels of Bax and cleaved caspase-3 were reduced, and the bcl-2 level was increased by miR-411-3p mimics, whereas the opposite results were found with the miR-411-3p inhibitor (Fig. 5g). The above observations indicated that miR-411-3p was highly expressed in OS, which contributed to OS cell growth and apoptosis inhibition.

MiR-411-3p promotes migration, invasion, EMT, and JAK2/STAT3 pathway activation in OS cells

As shown in Fig. 6a, b, the migration and invasion of OS cells were repressed by the miR-411-3p inhibitor but promoted by the miR-411-3p mimic. In addition, the miR-411-3p inhibitor inhibited EMT, as evidenced by the upregulation of E-cadherin and downregulation of N-cadherin, vimentin, MMP-2, and slug. However, these changes were reversed in the miR-411-3p mimic group (Fig. 6c). The p-JAK2 and p-STAT3 protein levels in OS cells were reduced by the miR-411-3p inhibitor but enhanced by the miR-411-3p mimic (Fig. 6d). In addition, transfection with miR-411-3p mimics downregulated SOCS1 protein abundance, whereas miR-411-3p inhibitor transfection upregulated SOCS1 protein abundance (Fig. 6d). These data demonstrated the promotive effects of miR-411-3p on OS cell metastasis in vitro.

Overexpression of miR-411-3p reverses the phenotypes of KIAA0087-overexpressing OS cells

Next, we evaluated whether miR-411-3p participated in the anticancer effects of KIAA0087 overexpression on OS cells.

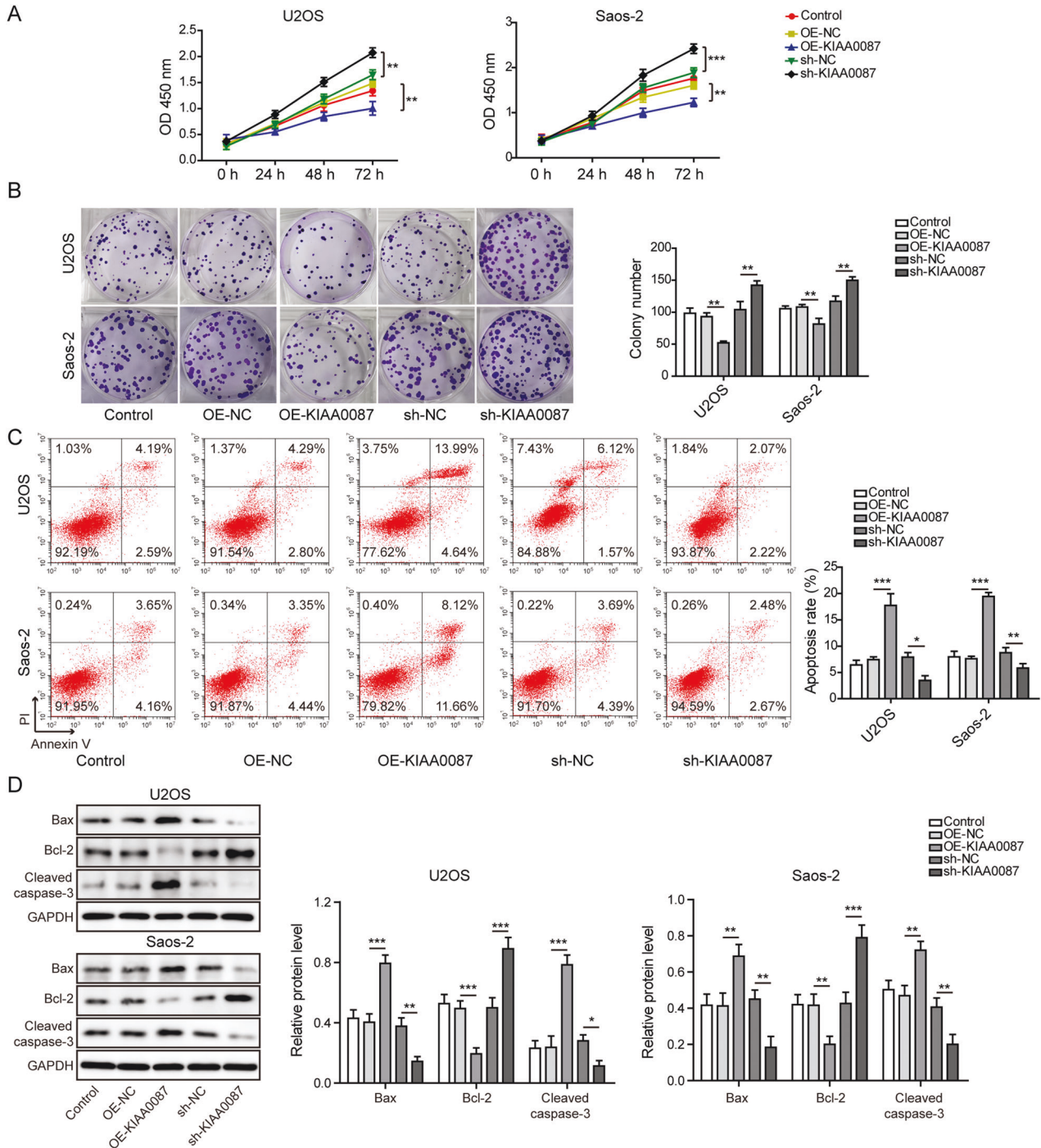


Fig. 2 Dysregulation of KIAA0087 affects the proliferation and apoptosis of OS cells. **a** CCK-8 assay determined the proliferation of OS cells. **b** Colony formation assay for evaluating the growth of OS cells. **c** Flow cytometry for testing the apoptotic rate of OS cells. **d** The protein levels of Bax, bcl-2, and cleaved caspase-3 in OS cells were determined by western blotting. * $p < 0.05$, ** $p < 0.01$, and *** $p < 0.001$.

As determined by RT-qPCR, the decreased expression of miR-411-3p in KIAA0087-overexpressing OS cells was effectively reversed by miR-411-3p mimics (Supplementary Fig. 2a). Importantly, miR-411-3p mimics remarkably abolished the effects of KIAA0087 overexpression on proliferation (Supplementary Fig. 2b, c), apoptosis (Supplementary Fig. 2d), migration (Supplementary Fig. 3a), and invasion of OS cells (Supplementary Fig. 3b). In addition, the weakened EMT mediated by KIAA0087 overexpression was restored by miR-411-3p overexpression (Supplementary Fig. 3c). As shown in Supplementary Fig. 3d, the levels of

phosphorylated JAK2 and STAT3 were significantly restricted by KIAA0087 overexpression but restored by miR-411-3p mimics. Additionally, the increased SOCS1 protein induced by KIAA0087 was reversed by miR-411-3p mimics (Supplementary Fig. 3d). Therefore, miR-411-3p partially counteracted the antitumor effects induced by KIAA0087 overexpression.

MiR-411-3p negatively regulates SOCS1 expression in OS cells

To further investigate the target gene of miR-411-3p, we preliminarily selected three candidates (SOCS1, RHOB, and

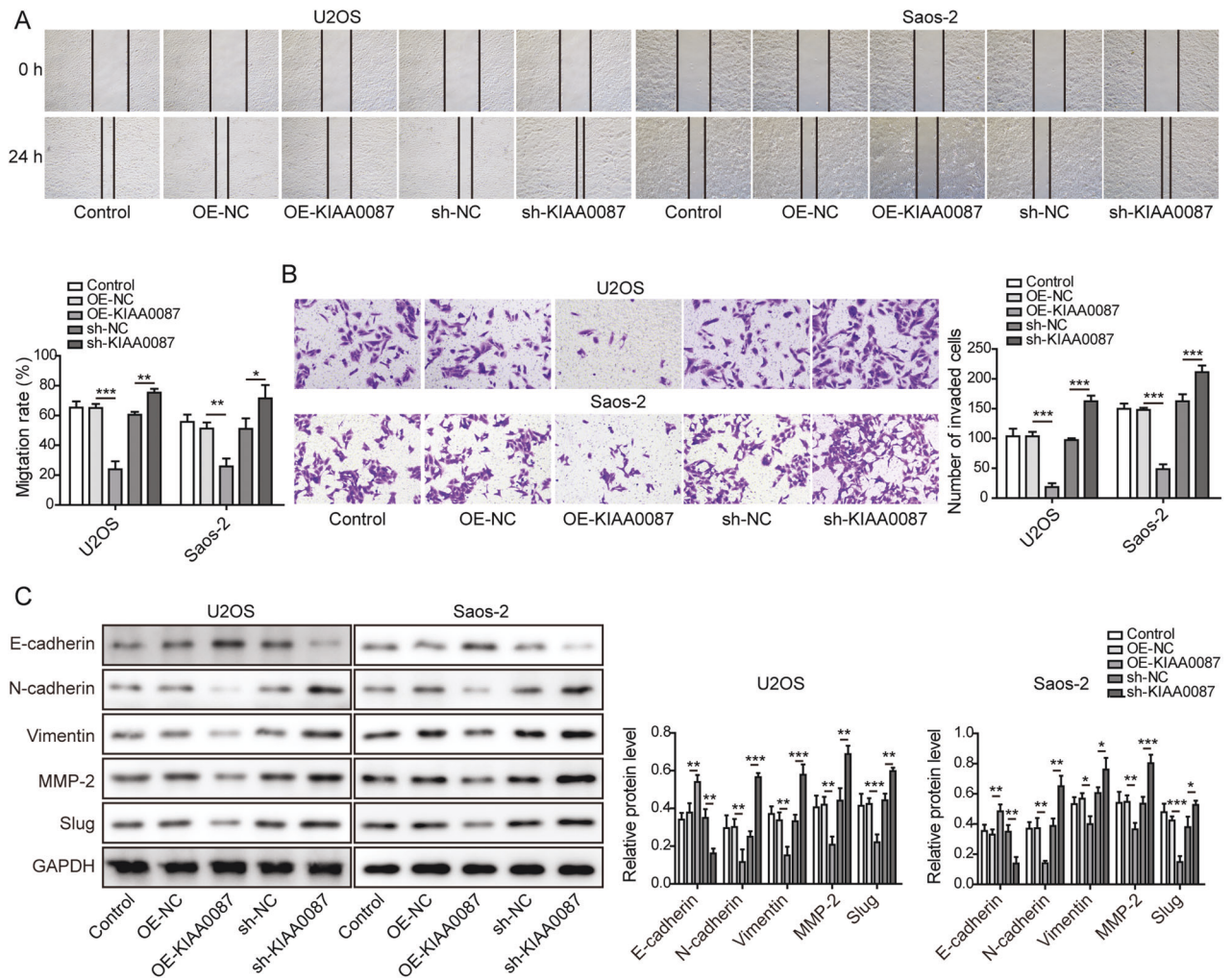


Fig. 3 Effect of KIAA0087 on the migration, invasion, and EMT of OS cells. **a** Wound healing assay for detecting the migration of OS cells. **b** Transwell assay for assessing the invasion of OS cells. **c** The protein levels of E-cadherin, N-cadherin, vimentin, MMP-2, and slug were assessed by western blotting. * $p < 0.05$, ** $p < 0.01$, and *** $p < 0.001$.

XRN1) according to prediction ranking and gene function. Further experiments showed that the change in SOCS1 level was most obvious after overexpression or knockdown of miR-411-3p in OS cells (Fig. 7a). As presented in Fig. 7b, the protein level of SOCS1 was strikingly decreased in miR-411-3p-overexpressing cells but increased in miR-411-3p-depleted cells. Furthermore, the putative binding sites between SOCS1 and miR-411-3p were predicted by the StarBase database (Fig. 7c). Moreover, miR-411-3p mimics repressed and miR-411-3p inhibitor enhanced the luciferase activity of SOCS1-WT but not SOCS1-MUT (Fig. 7d). Down-regulation of SOCS1 in OS tumor tissues were validated by RT-qPCR assay (Fig. 7e). Consistently, SOCS1 was downregulated in various OS cells (Fig. 7f). A negative correlation between SOCS1 and miR-411-3p in OS tissues was also observed (Fig. 7g). These data revealed that miR-411-3p suppressed SOCS1 expression by binding to its 3'-UTR in OS cells.

Depletion of SOCS1 counteracts the anticancer effects of the miR-411-3p inhibitor on OS cells

Next, we explored whether miR-411-3p affected the malignant properties of OS cells by regulating SOCS1. RT-qPCR showed that depletion of SOCS1 evidently reversed the miR-411-3p inhibitor-induced promotion of SOCS1 mRNA in OS cells, while it did not affect miR-411-3p levels (Supplementary Fig. 4a, b). Additionally, the increased protein level of SOCS1 induced by

the miR-411-3p inhibitor was also abolished by SOCS1 inhibition (Supplementary Fig. 4c). Moreover, the miR-411-3p inhibitor weakened the proliferative, migratory, and invasive abilities but enhanced the apoptosis of OS cells, which was counteracted by silencing SOCS1 (Supplementary Fig. 4d–f and Supplementary Fig. 5a, b). Additionally, depletion of SOCS1 significantly restricted miR-411-3p inhibitor-mediated EMT inhibition in OS cells (Supplementary Fig. 5c). The reduced p-JAK2 and p-STAT3 levels in miR-411-3p inhibitor-transfected OS cells were partly restored by SOCS1 knockdown (Supplementary Fig. 5d). Collectively, miR-411-3p regulated the malignant phenotypes of OS cells through SOCS1.

KIAA0087 overexpression or miR-411-3p knockdown represses the growth and lung metastasis of OS cells in vivo

Finally, we assessed the roles of KIAA0087 or miR-411-3p in the carcinogenesis of OS in vivo. To achieve this, U2OS and Saos-2 cells stably infected with lentiviruses carrying KIAA0087 or miR-411-3p inhibitor were injected into nude mice. Obvious decreases in tumor weight and volume in the KIAA0087-overexpression or miR-411-3p-inhibition group were demonstrated (Fig. 8a, b). In addition, a lower Ki-67 expression level in tumor tissues was confirmed in the KIAA0087-overexpression or miR-411-3p-inhibition group (Fig. 8c). Overexpression of KIAA0087 or inhibition of miR-411-3p increased the E-cadherin

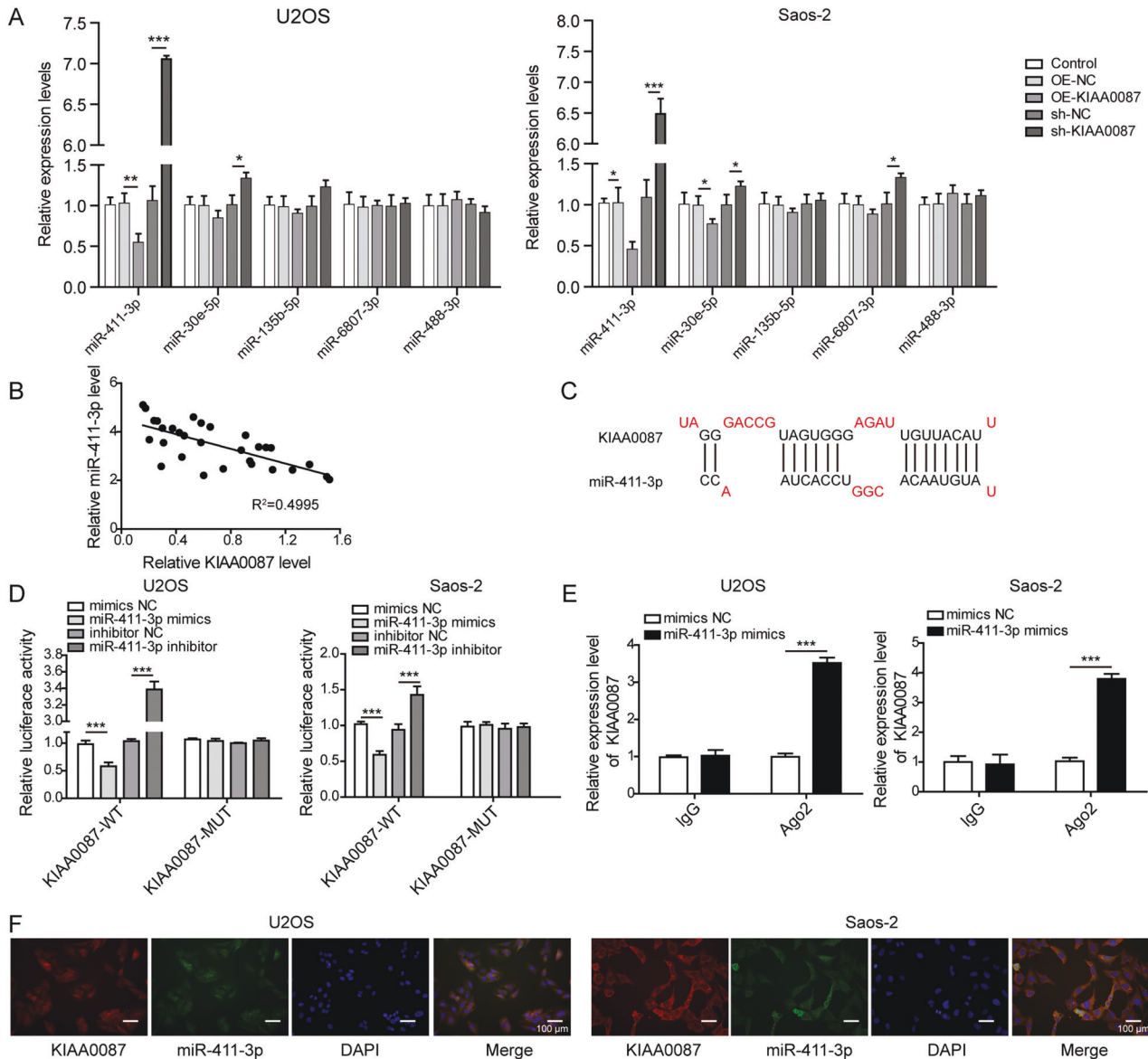


Fig. 4 KIAA0087 directly binds to miR-411-3p in OS cells. **a** rt-qPCR detected miR-411-3p, miR-30e-5p, miR-135b-5p, miR-6807-3p, and miR-488-3p expression after overexpression or inhibition of KIAA0087 in OS cells. **b** The correlation between KIAA0087 and miR-411-3p expression in the clinical OS samples was evaluated ($n = 30$). **c** Bioinformatic analysis of the specific binding regions between KIAA0087 and miR-411-3p. **d, e** The direct binding of KIAA0087 to miR-411-3p was validated by dual-luciferase reporter assay (**d**) and RIP assay (**e**). **f** The cytoplasmic colocalization of KIAA0087 and miR-411-3p in OS cells was observed by FISH. * $p < 0.05$, ** $p < 0.01$, and *** $p < 0.001$.

level but suppressed the N-cadherin expression level in tumor tissues, suggesting that the EMT process was repressed (Fig. 8d). In addition, KIAA0087 overexpression led to a decreased miR-411-3p expression level and an increased SOCS1 expression level in tumor tissues (Fig. 8e–h). Additionally, SOCS1 was upregulated in the miR-411-3p-inhibition group (Fig. 8g, h). Moreover, the in vivo metastatic capacity of OS cells was also assessed. As presented in Fig. 9a, H&E staining indicated that KIAA0087 overexpression or miR-411-3p inhibition strikingly reduced the area of metastatic OS cells in the lung tissues (Fig. 9a). The expression level of miR-411-3p declined, while SOCS1 expression was enhanced by KIAA0087 overexpression in the lung tissues (Fig. 9b–d). Accordingly, the expression of SOCS1 was enhanced in the lung tissues of the miR-411-3p-inhibition group (Fig. 9c, d). Collectively, the in vivo growth and lung metastasis of OS cells were suppressed by KIAA0087 overexpression or miR-411-3p inhibition.

DISCUSSION

Although improvement has been made in the 5-year survival rate of OS patients in recent years, recurrent or metastatic OS is still refractory to cancer treatments¹⁹. Therefore, identifying more effective therapies for treating refractory OS is urgently needed. Here, we uncovered the biological functions of a novel lncRNA, KIAA0087, in the progression of OS. We found that KIAA0087 was downregulated, but miR-411-3p was upregulated in OS tissues and cells, which facilitated the growth, metastasis, and EMT of OS cells in vitro and in vivo. Mechanistically, KIAA0087 sponged miR-411-3p to enhance SOCS1-mediated inactivation of the JAK2/STAT3 pathway. Our data demonstrated the potential value of KIAA0087 and miR-411-3p as effective targets for treating refractory OS.

In recent years, the biological functions of lncRNAs in cancers have attracted wide attention. Growing evidence has indicated that many lncRNAs are dysregulated in OS, which contributes to

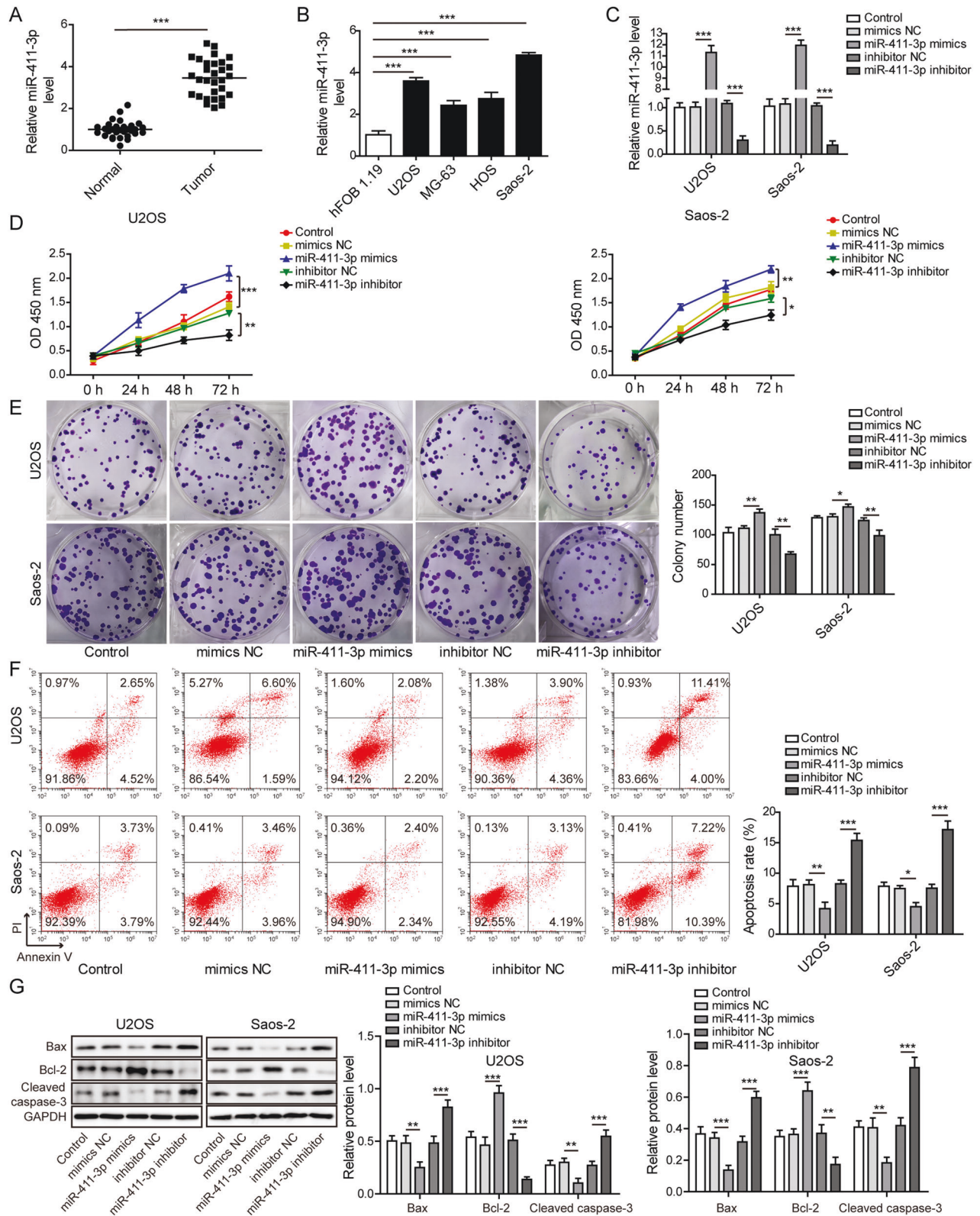


Fig. 5 Upregulation of miR-411-3p confers OS cell malignant growth. **a** RT-qPCR analysis was used to evaluate miR-411-3p levels in clinically normal and OS samples ($n = 30$). **b** RT-qPCR analysis was used to evaluate miR-411-3p levels in hFOB 1.19 and different OS cells (U2OS, Saos-2, MG-63, and HOS). **c** RT-qPCR assay was used to validate lentivirus-mediated overexpression or inhibition of miR-411-3p in OS cells. **d** CCK-8 assay determined the proliferation of OS cells. **e** Colony formation assay for evaluating the growth of OS cells. **f** Flow cytometry for testing the apoptotic rate of OS cells. **g** Western blot analysis of the protein levels of Bax, bcl-2, and cleaved caspase-3 in OS cells. * $p < 0.05$, ** $p < 0.01$, and *** $p < 0.001$.

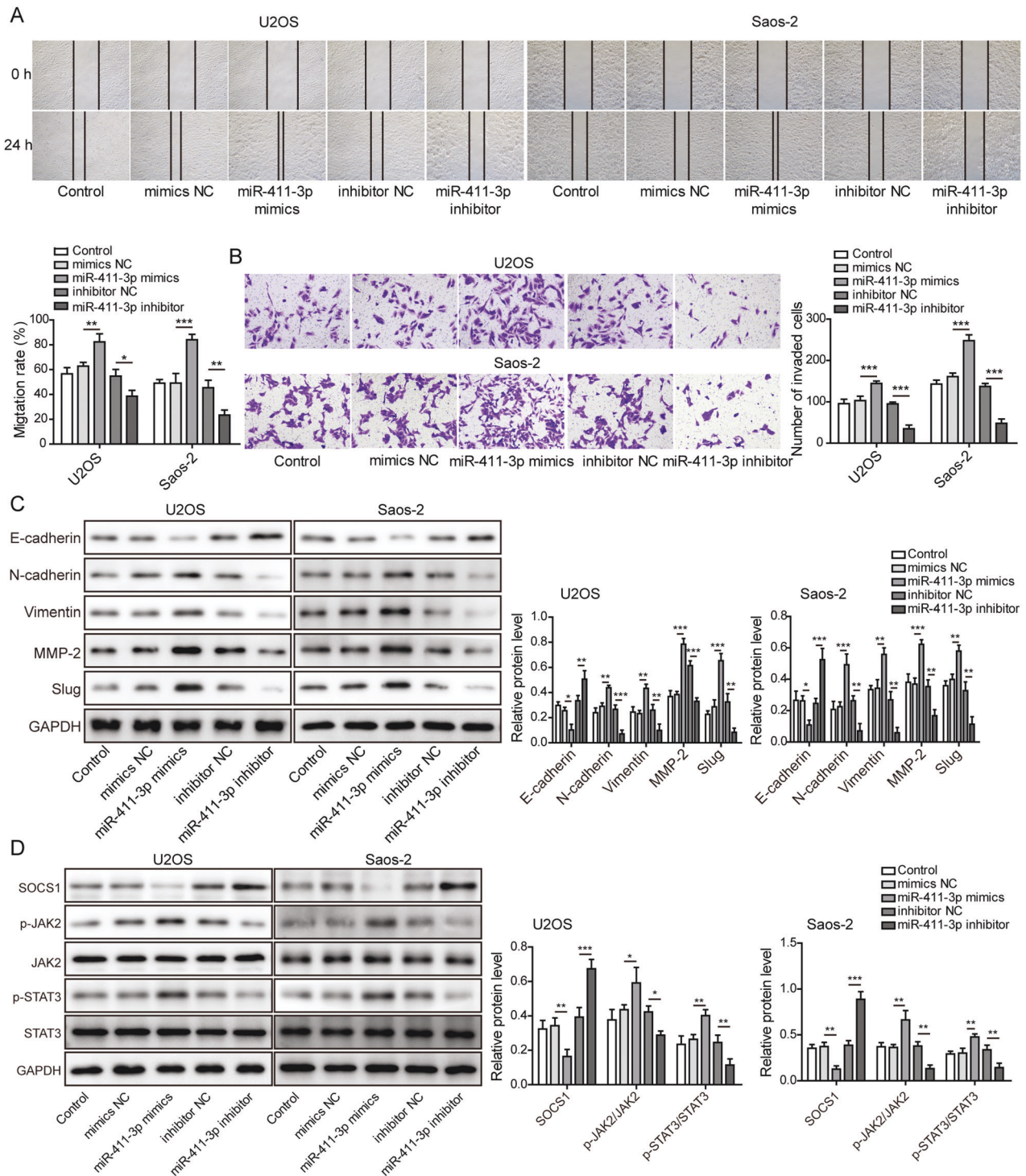


Fig. 6 MiR-411-3p overexpression promotes OS cell migration, invasion, and EMT. **a** Wound healing assay for detecting migration in OS cells. **b** Transwell assay for assessing the invasion of OS cells. **c** Western blotting for assessing the levels of EMT-related proteins, including E-cadherin, N-cadherin, vimentin, MMP-2, and slug. **d** Western blot analysis of the expression of SOCS1 and JAK2/STAT3 pathway component proteins. * $p < 0.05$, ** $p < 0.01$, and *** $p < 0.001$.

the malignant development of OS. For example, TUG1 is overexpressed in OS, and TUG1 silencing inhibits the proliferation and invasion of OS cells²⁰. Han et al. showed that lncRNA ATB facilitates OS cell growth and metastasis and can serve as a therapeutic target²¹. In our study, we focused on a novel lncRNA, KIAA0087. To date, limited studies have investigated the functions of KIAA0087 in OS. For the first time, we revealed that KIAA0087

was downregulated in OS tissues and cells, which was positively correlated with the TNM stage of OS patients. However, KIAA0087 expression was not significantly correlated with distant metastasis in OS patients, which might be caused by our limited sample size and individual and geographical differences in patients. EMT is a key process in the metastasis and progression of OS and plays pivotal roles in chemotherapy resistance, recurrence, and poor

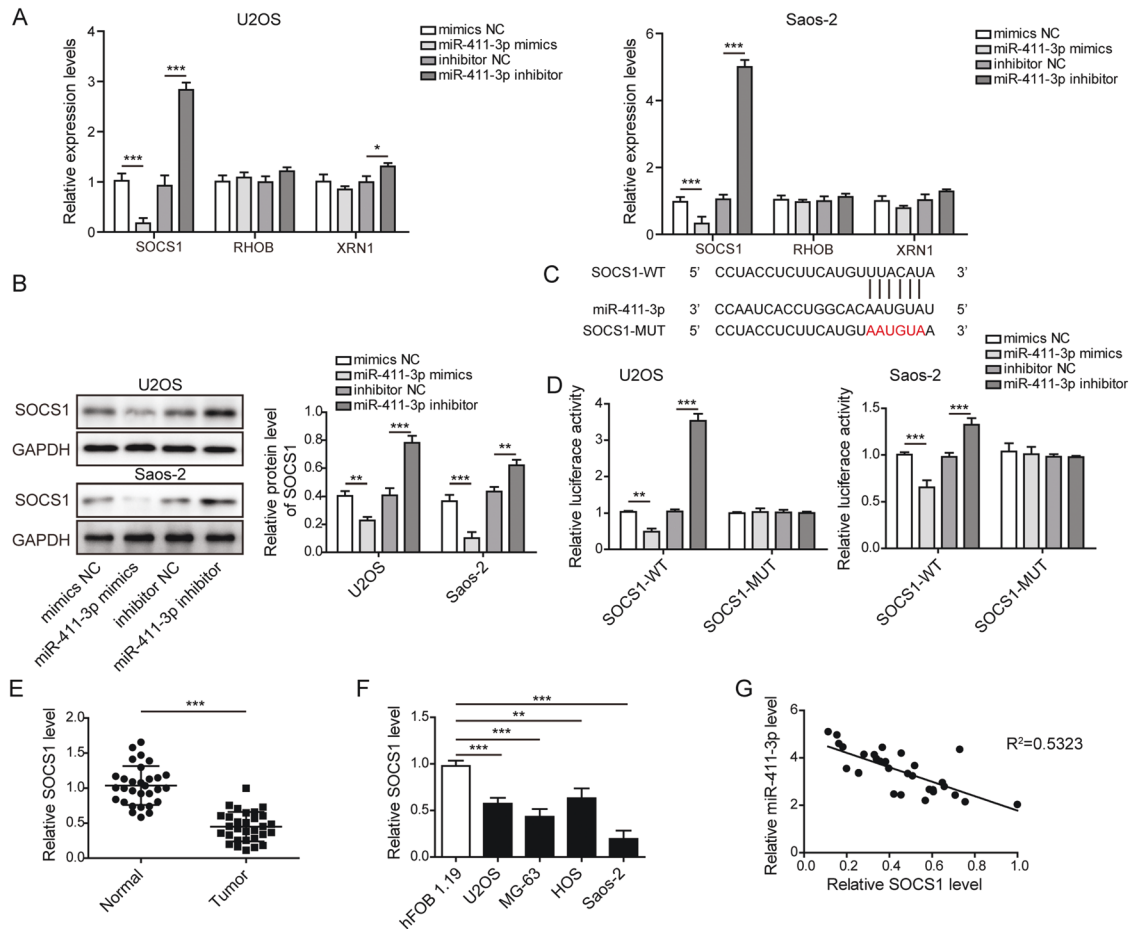


Fig. 7 SOCS1 is a target gene of miR-411-3p in OS cells. **a** The mRNA levels of SOCS1, RHOB, and XRN1 were detected by RT-qPCR after overexpression or inhibition of miR-411-3p in OS cells. **b** Western blotting was used to evaluate the protein level of SOCS1 in miR-411-3p mimic- or inhibitor-transfected OS cells. **c** Bioinformatic analysis of the potential miR-411-3p binding sites within the SOCS1 3'-UTR. **d** The direct binding of miR-411-3p to SOCS1 was confirmed by dual-luciferase reporter assay. **e** The expression level of SOCS1 in clinically normal and OS samples ($n = 30$) was determined by RT-qPCR. **f** RT-qPCR analysis of SOCS1 mRNA levels in various OS cells (U2OS, Saos-2, MG-63, and HOS). **g** Spearman correlation analysis of the correlation between the expression of miR-411-3p and SOCS1 in clinical OS samples ($n = 30$). * $p < 0.05$, ** $p < 0.01$, and *** $p < 0.001$.

prognosis^{22,23}. EMT induction is responsible for malignant cell metastasis during OS progression²⁴. Therefore, inhibiting the progression of EMT may be a potentially effective treatment for OS. In this study, we aimed to explore the underlying mechanism of EMT and metastasis in OS. Thus, a series of EMT-related signaling pathways that might be regulated by KIAA0087 were screened. We found that the JAK2/STAT3 pathway could be obviously affected by KIAA0087 in OS cells. Moreover, upregulation of KIAA0087 repressed OS cell growth, metastasis, and EMT and triggered apoptosis *in vitro* and *in vivo*. These observations suggest that KIAA0087 is a tumor suppressor in OS.

We further explored the underlying mechanisms by which KIAA0087 regulates the development of OS. By bioinformatics analysis, five target miRNAs (miR-30e-5p, miR-135b-5p, miR-6807-3p, miR-488-3p, and miR-411-3p) of KIAA0087 were screened preliminarily. Further results showed that the change in miR-411-3p level was apparently most pronounced after regulation by KIAA0087 in OS cells. Thus, miR-411-3p was a focus of this study. In previous studies, miR-411-3p has been reported to affect tumor development. For instance, miR-411-3p, as a target of lncRNA TTN-AS1, is involved in the pathogenesis of oral squamous cell carcinoma²⁵. Here, we provided the first evidence that miR-411-3p upregulation promoted the malignant properties of OS cells. More importantly, we found that miR-411-3p was elevated by KIAA0087

knockdown but reduced by KIAA0087 overexpression. In addition, the direct interaction between miR-411-3p and KIAA0087 was validated by dual-luciferase, RIP, and FISH assays. Further rescue experiments demonstrated that miR-411-3p mimics effectively reversed the antitumor effects of KIAA0087 overexpression on OS cells. Therefore, KIAA0087 downregulation promoted tumorigenesis of OS via direct upregulation of miR-411-3p expression. Our research team reported for the first time that KIAA0087 could sponge miR-411-3p.

We further selected SOCS1 as the target gene of miR-411-3p because the miR-411-3p-mediated level change in SOCS1 was the most pronounced. SOCS1 is downregulated in OS tissues and cells¹⁸. SOCS1 has been shown to repress EMT-mediated metastasis and invasion in cervical cancer²⁶. David et al reported that SOCS1 suppressed the metastatic progression of colorectal cancer by reversing EMT²⁷. Consistent with these studies, we found a reduction in SOCS1 expression in OS tissues and cells, which negatively correlated with miR-411-3p expression in OS patients. More importantly, SOCS1 expression was enhanced by a miR-411-3p inhibitor but reduced by miR-411-3p mimics. The direct binding between miR-411-3p and SOCS1 was confirmed by dual-luciferase assay. Furthermore, silencing SOCS1 reversed the antitumor effects of the miR-411-3p inhibitor on OS cells. Therefore, miR-411-3p affected OS progression by targeting

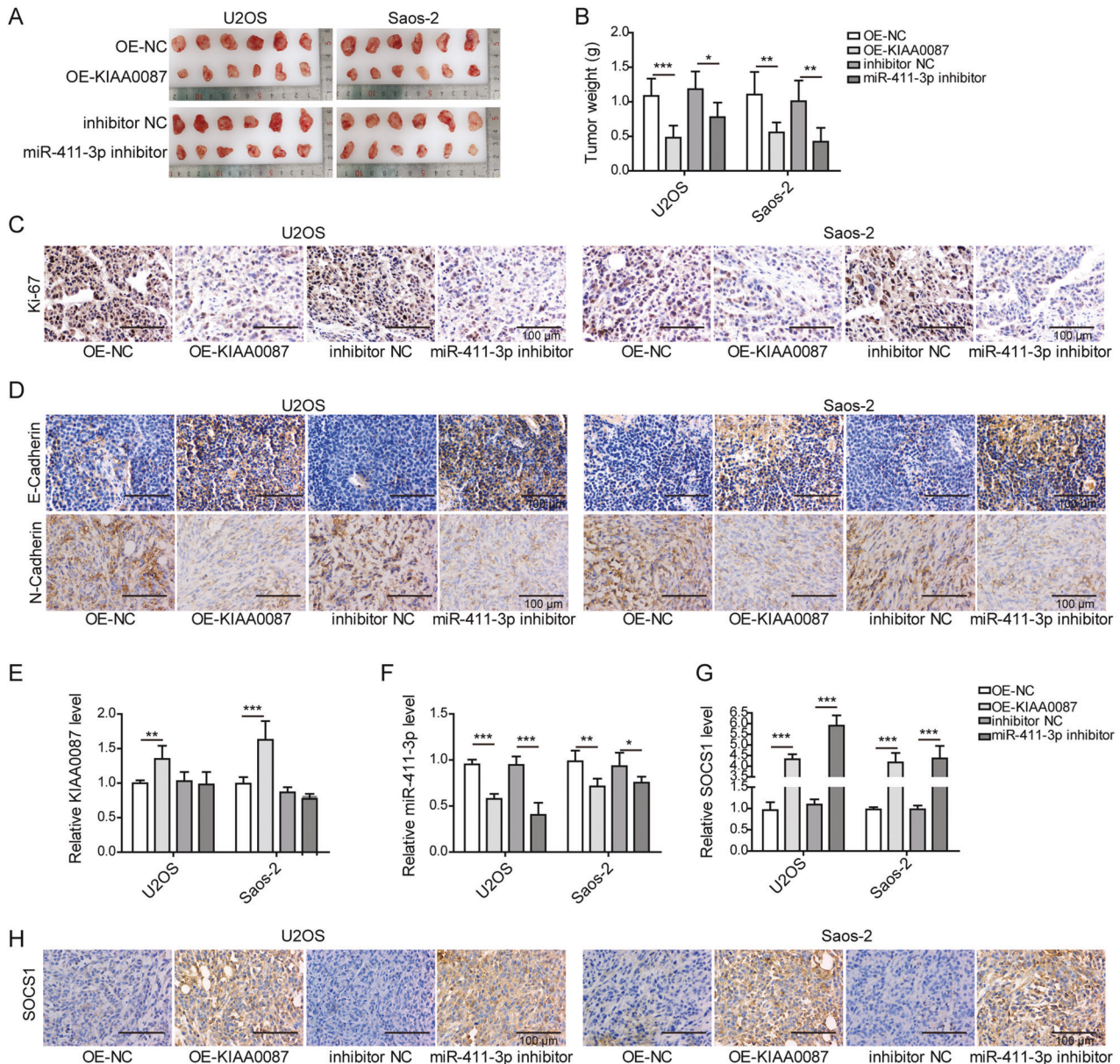


Fig. 8 KIAA0087 overexpression or miR-411-3p knockdown disrupts tumor growth in vivo. **a, b** Xenograft tumors (**a**) and quantitative results (**b**) of tumor weight from various groups. **c** Ki-67 expression in tumor tissues was determined by immunohistochemical staining. **d** E-cadherin and N-cadherin expression in tumor tissues was determined by immunohistochemical staining. **e–g** RT-qPCR for determining KIAA0087 (**e**), miR-411-3p (**f**), and SOCS1 (**g**) expression in tumor tissues. **h** SOCS1 expression in tumor tissues was detected by immunohistochemical staining. * $p < 0.05$, ** $p < 0.01$, and *** $p < 0.001$.

SOCS1. This is the first evidence of the direct link between miR-411-3p and SOCS1 in OS.

SOCS1 is a potent suppressor of the JAK2/STAT3 pathway through proteasomal degradation of JAK2²⁶. JAK2 is an important member of the JAK family, which regulates various biological functions, such as proliferation, migration, and apoptosis²⁸. The phosphorylation of JAK2 can lead to the activation of STAT3²⁹. Mounting evidence has demonstrated that the activation of the JAK2/STAT3 pathway participates in the growth and metastasis of OS^{30–32}. STAT3 can promote the EMT process in tumors by enhancing vimentin expression³³. In the present study, the activation of the JAK2/STAT3 pathway was suppressed by forced expression of KIAA0087 or miR-411-3p inhibitor. Therefore, the JAK2/STAT3 pathway participated in KIAA0087/miR-411-3p/SOCS1 axis-mediated tumorigenesis of OS.

We are aware that this study has several limitations. First, we did not investigate what caused the downregulation of KIAA0087 in OS. Second, the identification of potential EMT-related signaling networks regulated by KIAA0087 using bioinformatics data may expand the pathological mechanisms of OS development. Third, we mainly explored the function and related mechanisms of KIAA0087 in the EMT and metastasis of OS cells. Other biological functions of KIAA0087 in OS remain unclear and need to be explored in future studies. Nevertheless, this research is the first to reveal that KIAA0087 promotes SOCS1-mediated inactivation of the JAK2/STAT3 pathway by sponging miR-411-3p, which suppresses the growth and metastasis of OS cells in vitro and in vivo. Our findings provide new insights into molecular mechanisms of OS oncogenesis and a potential therapeutic target.

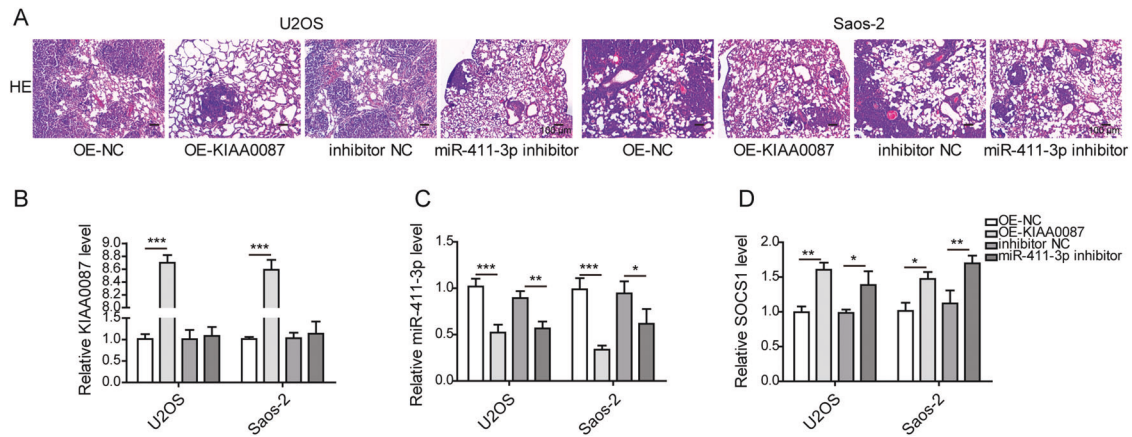


Fig. 9 KIAA0087 overexpression or miR-411-3p inhibition suppresses lung metastasis in vivo. **a** HE staining for evaluating metastatic tumor cells in lung tissues. **b–d** RT-qPCR for detecting KIAA0087 (**b**), miR-411-3p (**c**), and SOCS1 (**d**) expression in the lung tissues of nude mice. * $p < 0.05$, ** $p < 0.01$, and *** $p < 0.001$.

REFERENCES

- Caudill, J. S. & Arndt, C. A. Diagnosis and management of bone malignancy in adolescence. *Adolesc. Med. State Art. Rev.* **18**, 62–78 (2007).
- Ottaviani, G. & Jaffe, N. The epidemiology of osteosarcoma. *Cancer Treat. Res.* **152**, 3–13 (2009).
- Tsakamoto, S., Errani, C., Angelini, A. & Mavrogenis, A. F. Current treatment considerations for osteosarcoma metastatic at presentation. *Orthopedics* **43**, e345–e358 (2020).
- Qiu, S., Tao, L. & Zhu, Y. Marital status and survival in osteosarcoma patients: an analysis of the surveillance, epidemiology, and end results (SEER) database. *Med. Sci. Monit.* **25**, 8190–8203 (2019).
- Lu, K. H. Molecular and cellular mechanisms of melatonin in osteosarcoma. *Cells* **8**, 1618 (2019).
- Singh, S. & Chakrabarti, R. Consequences of EMT-driven changes in the immune microenvironment of breast cancer and therapeutic response of cancer cells. *J. Clin. Med.* **8**, 642 (2019).
- Xing, S. et al. Down-regulation of PDGFRbeta suppresses invasion and migration in osteosarcoma cells by influencing epithelial-mesenchymal transition. *FEBS Open Bio* **10**, 1748–1757 (2020).
- Zheng, H. L. et al. Characterization of lncRNA SNHG22 as a protector of NKIRAS2 through miR-4492 binding in osteosarcoma. *Aging (Albany NY)* **12**, 18571–18587 (2020).
- Xu, J. et al. Distinct expression profile of lncRNA in endometrial carcinoma. *Oncol. Rep.* **36**, 3405–3412 (2016).
- Militello, G. et al. Screening and validation of lncRNAs and circRNAs as miRNA sponges. *Brief Bioinform.* **18**, 780–788 (2017).
- Garzon, R., Calin, G. A. & Croce, C. M. MicroRNAs in cancer. *Annu. Rev. Med.* **60**, 167–179 (2009).
- Yi, X., Wang, Y. & Xu, S. MiR-455-3p downregulation facilitates cell proliferation and invasion and predicts poor prognosis of osteosarcoma. *J. Orthop. Surg. Res.* **15**, 454 (2020).
- Gourbault, O. & Llobat, L. MicroRNAs as biomarkers in canine osteosarcoma: a new future? *Vet. Sci.* **7**, 146 (2020).
- Liu, J., Wu, S., Xie, X., Wang, Z. & Lei, Q. The role of significantly deregulated MicroRNAs in osteosarcoma based on bioinformatic analysis. *Technol. Health Care* **29**, 333–341 (2020).
- Beaurivage, C. et al. SOCS1 in cancer: an oncogene and a tumor suppressor. *Cytokine* **82**, 87–94 (2016).
- Zhang, X. H. et al. Association between methylation of tumor suppressor gene SOCS1 and acute myeloid leukemia. *Oncol. Rep.* **40**, 1008–1016 (2018).
- Hashimoto, M. et al. Silencing of SOCS1 in macrophages suppresses tumor development by enhancing antitumor inflammation. *Cancer Sci.* **100**, 730–736 (2009).
- Gong, H. L. et al. MicroRNA-29a suppresses the invasion and migration of osteosarcoma cells by regulating the SOCS1/NF-kappaB signalling pathway through negatively targeting DNMT3B. *Int. J. Mol. Med.* **44**, 1219–1232 (2019).
- Bielack, S. S. et al. Prognostic factors in high-grade osteosarcoma of the extremities or trunk: an analysis of 1,702 patients treated on neoadjuvant cooperative osteosarcoma study group protocols. *J. Clin. Oncol.* **20**, 776–790 (2002).
- Wang, H., Yu, Y., Fan, S. & Luo, L. Knockdown of long noncoding RNA TUG1 inhibits the proliferation and cellular invasion of osteosarcoma cells by sponging miR-153. *Oncol. Res.* **26**, 665–673 (2018).
- Han, F., Wang, C., Wang, Y. & Zhang, L. Long noncoding RNA ATB promotes osteosarcoma cell proliferation, migration and invasion by suppressing miR-200s. *Am. J. Cancer Res.* **7**, 770–783 (2017).
- Li, R., Ruan, Q., Zheng, J., Zhang, B. & Yang, H. LINC01116 promotes doxorubicin resistance in osteosarcoma by epigenetically silencing miR-424-5p and inducing epithelial-mesenchymal transition. *Front. Pharmacol.* **12**, 632206 (2021).
- Zeng, S. X. et al. High expression of TRIM29 (ATDC) contributes to poor prognosis and tumor metastasis by inducing epithelialmesenchymal transition in osteosarcoma. *Oncol. Rep.* **38**, 1645–1654 (2017).
- Shao, S. et al. Tspan9 induces EMT and promotes osteosarcoma metastasis via activating FAK-Ras-ERK1/2 pathway. *Front. Oncol.* **12**, 774988 (2022).
- Fu, S. W. et al. lncRNA TTN-AS1 promotes the progression of oral squamous cell carcinoma via miR-411-3p/NFAT5 axis. *Cancer Cell Int.* **20**, 415 (2020).
- Zeng, Y. T., Liu, X. F., Yang, W. T. & Zheng, P. S. REX1 promotes EMT-induced cell metastasis by activating the JAK2/STAT3-signaling pathway by targeting SOCS1 in cervical cancer. *Oncogene* **38**, 6940–6957 (2019).
- David, M. et al. Suppressor of cytokine signaling 1 modulates invasion and metastatic potential of colorectal cancer cells. *Mol. Oncol.* **8**, 942–955 (2014).
- Groner, B. & von Manstein, V. Jak Stat signaling and cancer: opportunities, benefits and side effects of targeted inhibition. *Mol. Cell. Endocrinol.* **451**, 1–14 (2017).
- Li, S. et al. RUNX3 protects against acute lung injury by inhibiting the JAK2/STAT3 pathway in rats with severe acute pancreatitis. *Eur. Rev. Med. Pharmacol. Sci.* **23**, 5382–5391 (2019).
- Chen, J. & Chen, Z. Downregulation of miR-19a inhibits the proliferation and promotes the apoptosis of osteosarcoma cells by regulating the JAK2/STAT3 pathway. *Oncol. Lett.* **20**, 173 (2020).
- Ge, X. et al. Exosomal transfer of LCP1 Promotes Osteosarcoma Cell Tumorigenesis and Metastasis by Activating the JAK2/STAT3 signaling pathway. *Mol. Ther. Nucleic Acids* **21**, 900–915 (2020).
- Huang, H. et al. ML264 inhibits osteosarcoma growth and metastasis via inhibition of JAK2/STAT3 and WNT/beta-catenin signalling pathways. *J. Cell. Mol. Med.* **24**, 5652–5664 (2020).
- Cui, Y. et al. STAT3 regulates hypoxia-induced epithelial mesenchymal transition in oesophageal squamous cell cancer. *Oncol. Rep.* **36**, 108–116 (2016).

FUNDING

This work was supported by Natural Science Foundation of Hunan Province (2022JJ40218), Scientific Research Program of the Hunan Provincial Health Commission (No. 202204073200 and No. 202204073644) and the Scientific Research Project of the Hunan Provincial Education Department (No. 21B0042 and No. 21B0031).

COMPETING INTERESTS

The authors declare no competing interests.

ETHICS APPROVAL AND CONSENT TO PARTICIPATE

Clinical OS tissues and matched normal tissues were collected from 30 OS patients during surgery at Hunan Provincial People's Hospital (The First Affiliated

Hospital of Hunan Normal University). The collected samples were snap-frozen in liquid nitrogen and preserved at -80°C . No patients had previously undergone chemoradiotherapy, and all patients signed written informed consent. Our experiments were approved by the Ethics Committee of Hunan Provincial People's Hospital (The First Affiliated Hospital of Hunan Normal University). The animal experiments were approved by the Animal Ethics Committee of Hunan Provincial People's Hospital (The First Affiliated Hospital of Hunan Normal University).

ADDITIONAL INFORMATION

Supplementary information The online version contains supplementary material available at <https://doi.org/10.1038/s12276-023-00972-8>.

Correspondence and requests for materials should be addressed to Ming Zeng.

Reprints and permission information is available at <http://www.nature.com/reprints>

Publisher's note Springer Nature remains neutral with regard to jurisdictional claims in published maps and institutional affiliations.



Open Access This article is licensed under a Creative Commons Attribution 4.0 International License, which permits use, sharing, adaptation, distribution and reproduction in any medium or format, as long as you give appropriate credit to the original author(s) and the source, provide a link to the Creative Commons license, and indicate if changes were made. The images or other third party material in this article are included in the article's Creative Commons license, unless indicated otherwise in a credit line to the material. If material is not included in the article's Creative Commons license and your intended use is not permitted by statutory regulation or exceeds the permitted use, you will need to obtain permission directly from the copyright holder. To view a copy of this license, visit <http://creativecommons.org/licenses/by/4.0/>.

© The Author(s) 2023